Conf-9306170--1

ISOLATION OF A PIEZORESISTIVE ACCELEROMETER USED IN HIGH ACCELERATION TESTS*

Vesta I. Bateman
Fred A. Brown
Neil T. Davie
Sandia National Laboratories
Albuquerque, New Mexico 87185

RECEIVED
MAY 24 1993
OSTI

ABSTRACT

Both uniaxial and triaxial shock isolation techniques for a piezoresistive accelerometer have been developed for pyroshock and impact tests. The uniaxial shock isolation technique has demonstrated acceptable characteristics for a temperature range of -50°F to +186°F and a frequency bandwidth of DC to 10 kHz. The triaxial shock isolation technique has demonstrated acceptable results for a temperature range of -50°F to 70°F and a frequency bandwidth of DC to 10 kHz. These temperature ranges, that are beyond the accelerometer manufacturer's operational limits of -30°F and +150°F, required the calibration of accelerometers at high shock levels and at the temperature extremes of -50°F and +160°F. The purposes of these calibrations were to insure that the accelerometers operated at the field test temperatures and to provide an accelerometer sensitivity at each test temperature. Since there is no NIST-traceable (National Institute of Standards and Technology traceable) calibration capability at shock levels of 5,000 g - 15,000 g for the temperature extremes of -50°F and +160°F, a method for calibrating and certifying the Hopkinson bar with a transfer standard was developed. Time domain and frequency domain results are given that characterize the Hopkinson bar. The NIST-traceable accuracy for the standard accelerometer in shock is ±5%. The Hopkinson bar has been certified by the Sandia Secondary Standards Division with an uncertainty of 6%.

INTRODUCTION

Sandia National Laboratories (SNL) conduct impact testing for a variety of structures as discussed in other papers [1,2]. During an impact test, metal to metal contact may occur within the structure and produce high frequency, high amplitude shocks. The high frequency portion of this transient vibration has been observed to excite an accelerometer into resonance even though this resonance exceeds 350 kHz. An accelerometer may fail in this situation. Even if the accelerometer does not fail, the amplitude of the resonating accelerometer response can be so large that the data are clipped and rendered useless. If the data are not clipped, a digital filter must be applied to eliminate undesirable accelerometer resonant response. In

*This work was performed at Sandia National Laboratories and was supported by the U.S. Department of Energy under Contract DE-AC04-76-DP00789.

MASTER
DISTRIBUTION OF THIS DOCUMENT IS UNLIMITED

DISCLAIMER

This report was prepared as an account of work sponsored by an agency of the United States Government. Neither the United States Government nor any agency thereof, nor any of their employees, makes any warranty, express or implied, or assumes any legal liability or responsibility for the accuracy, completeness, or usefulness of any information, apparatus, product, or process disclosed, or represents that its use would not infringe privately owned rights. Reference herein to any specific commercial product, process, or service by trade name, trademark, manufacturer, or otherwise does not necessarily constitute or imply its endorsement, recommendation, or favoring by the United States Government or any agency thereof. The views and opinions of authors expressed herein do not necessarily state or reflect those of the United States Government or any agency thereof.

anticipation of accelerometers' resonating during a test, the data channels may be set to accomodate the large amplitude of the accelerometer resonance. The result is usually an unacceptably small signal to noise ratio. If possible, it is more desirable to prevent excitation of the accelerometer resonance. This may be accomplished by mechanically isolating the accelerometer from the high frequency excitation without degrading the transducer response in the bandwidth of interest.

In the past, several techniques have been used at Sandia National Laboratories to mechanically isolate accelerometers and instrumentation packages containing accelerometers from high frequency, high amplitude shock environments. These techniques include various configurations of adiprene, polysulfide rubber, water soluble wax, and urethane rubber [3,4,5]. The techniques have been successful in mechanically isolating the accelerometers but have a limited, useable frequency range of 2 kHz or less. The useable frequency range is specified as those frequencies for which the sensitivity deviation is $\pm 5\%$ or less. In one application, a mechanical isolator was combined with an electrical analog filter, tuned for the isolator resonance, to achieve a useable frequency range of 10 kHz. A commercially available, mechanical isolator has also been evaluated. However, this isolator exhibited nonlinear behavior over its acceleration capability of 1500 g. A commercial piezoelectric accelerometer with integral electronics and mechanical isolation is available but is generally not used in our field testing because of signal conditioning requirements, cable-whip and zero-shift problems, and a limited useable frequency range of about 1 kHz.

A bandwidth of 10 kHz is needed for many applications because more sophisticated analyses are being performed with the field data. The isolation techniques were designed and evaluated for the desired bandwidth of 10 kHz. These techniques are used with a piezoresistive accelerometer which is frequently used for field tests of various high reliability structures which must withstand severe shock environments. The piezoresistive accelerometer has several desirable characteristics: DC response, low power requirements, minimal zero shift, and high resonant frequency. One undesirable characteristic is that the piezoresisitive accelerometer is undamped. A high frequency input causes it to resonate, and the resulting large amplitude may exceed the measuring capability of the instrumentation system. The resonant behavior is prevented with a mechanical isolator that has a damped resonance between the upper limit of the useable frequency range and the accelerometer's resonance. For example, the uniaxial isolator assembly has a damped resonance at about 50 kHz. This resonance allows attenuation of frequency input to the accelerometer above 50 kHz, and is useable for the piezoresistive accelerometer models with ranges equal to or greater than 6,000 g.

There are several goals in the design of a shock isolation technique. Primarily, the technique must have repeatable response characteristics. Secondly, the technique must allow calibration of the shock isolated accelerometer assembly prior to and after a field test. Lastly, the

technique must show linear amplitude and frequency characteristics. These goals have been achieved with the mechanical isolators developed at Sandia National Laboratories for a piezoresistive accelerometer [6,7]. The uniaxial shock isolation technique has demonstrated acceptable characteristics for a temperature range of -50°F to +186°F and a frequency bandwidth of DC to 10 kHz. The triaxial shock isolation technique has demonstrated acceptable results for a temperature range of -50°F to 70°F and a frequency bandwidth of DC to 10 kHz. Additionally, these characteristics have been verified by the calibration of the Hopkinson bar used for testing of the isolation techniques [8]. This paper will discuss the testing that has been conducted to demonstrate the performance of the isolation techniques and the calibration of the Hopkinson bar that has been performed to verify the results.

UNIAXIAL AND TRIAXIAL ISOLATION DESIGNS AND CALIBRATION

The uniaxial and triaxial isolation techniques are shown in Figure 1. The uniaxial technique consists of an aluminum disk that has a slot for the accelerometer. The disk is divided into two halves that are held together by two screws. A layer of polysulfide rubber compound (PRC-1422) is positioned on each side of the accelerometer in the slot. Brass locator pins (not shown) hold the PRC-1422 and accelerometer layers in place in the slot. An integral stud on the bottom of the disk is used to attach the uniaxial isolator assembly to the test structure (25 in-lbs mounting torque). Shrink tubing is used on the brass pins in the disk technique to prevent metal to metal contact during lateral shocks.

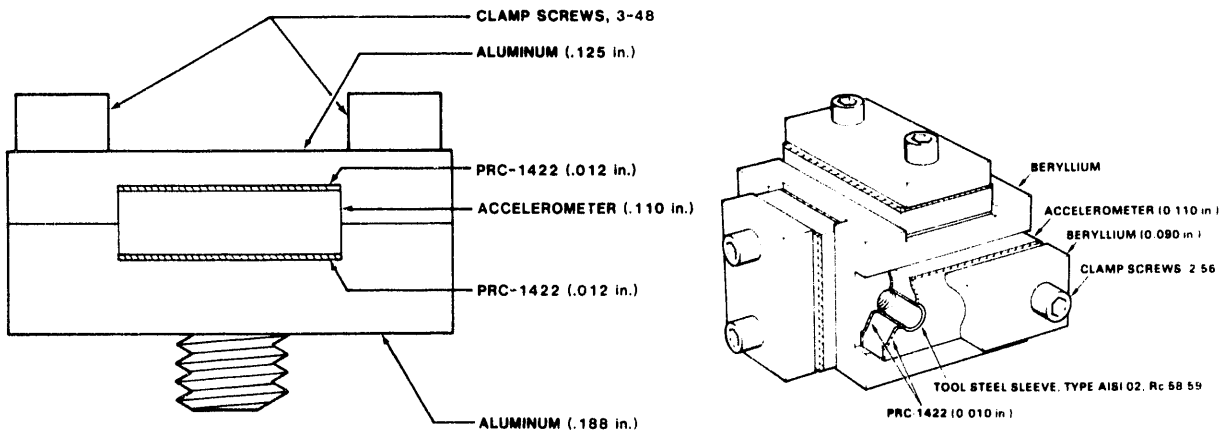

a) Uniaxial Isolation Technique **b) Triaxial Isolation Technique**

Figure 1: Uniaxial and Triaxial Isolation Techniques for a Piezoresistive Accelerometer.

The triaxial isolation technique, also shown in Figure 1, consists of a 0.6 in. cube of either 7075 aluminum or beryllium that has been machined with a slot on each of three orthogonal faces. The piezoresistive accelerometers are mounted in the slots with a layer of PRC-1422 on either side in the same manner as the uniaxial isolation technique. Hardened steel sleeves are

covered with shrink tubing to prevent metal-to-metal contact and are pressed into the mounting holes in the accelerometer. The sleeves are 0.125 in. long and provide correct spacing between the top plate and the bottom of the slot so that a consistent compression is maintained on the elastic material, PRC-1422. The plate, accelerometer, and layers of PRC-1422 are held in place with 2-56 screws that are torqued to 60 in-oz. A torque of 40 in-lbs is used for the triaxial isolation assembly mounting stud.

All accelerometers in this study were calibrated in the Sandia Calibration Laboratory using three methods: 1) shaker calibration; 2) centrifuge calibration; and 3) dropball calibration. The three methods are traceable to the National Institute of Standards and Technology, NIST, formerly NBS as described elsewhere [6]. Two commercially available mechanical isolators were evaluated using 6000 g piezoresistive accelerometers. Although the dropball and centrifuge calibrations were acceptable, both commercial isolators showed a deviation of 36% at 5 kHz in the shaker calibration at 5 g input as shown in Figure 2a. A uniaxial isolator assembly calibration at 30 g input is also shown for comparison. The damped resonance at 5 kHz is in agreement with the manufacturer's specifcations for the commercial isolator. The shaker data indicates that the useable frequency range, defined as less than 5% deviation from the 100 Hz reference, is about 1 kHz. Additionally, the commercial assemblies were evaluated on the Hopkinson bar, described in a later section, at two levels of 500 g and 1500 g with a pulse duration of 100 μs. These tests showed amplitude nonlinearities in the commercial isolator.

Figure 2b shows a shaker calibration at 30 g input for a uniaxial isolator assembly. This isolator had a sensitivity variation of less than $\pm$0.5% for the $\pm$5000 g centrifuge calibration (not shown). Figure 2c depicts a dropball calibration of the uniaxial isolator. Since the isolators were satisfactorily calibrated by all three methods, a more detailed evaluation of the shock isolation techniques was undertaken to investigate the linearity of amplitude and frequency characteristics on the Hopkinson bar in the Sandia Shock Laboratory.

HOPKINSON BAR CONFIGURATIONS FOR CHARACTERIZATION OF SHOCK ISOLATION TECHNIQUES

Accelerometer calibrations at temperatures other than ambient can only be conducted with the shaker due to limitations of existing equipment at the SNL Secondary Standards Lab. For shock accelerometers, it is desirable to calibrate with the dropball or with another shock producing technique such as the Hopkinson bar. The Hopkinson bar easily lends itself to temperature conditioning because the end of the bar, where the accelerometer is mounted, is simply inserted into a temperature chamber. For this reason, shock calibrations for the shock isolation techniques at the temperature extremes of -50°F and +186°F were conducted with a Hopkinson bar located in the SNL Shock Laboratory. The configuration for a normal input is shown in Figure 3. Normal input in this configuration is an input that is normal to the mounting surface and is also parallel to the integral mounting stud. Both the

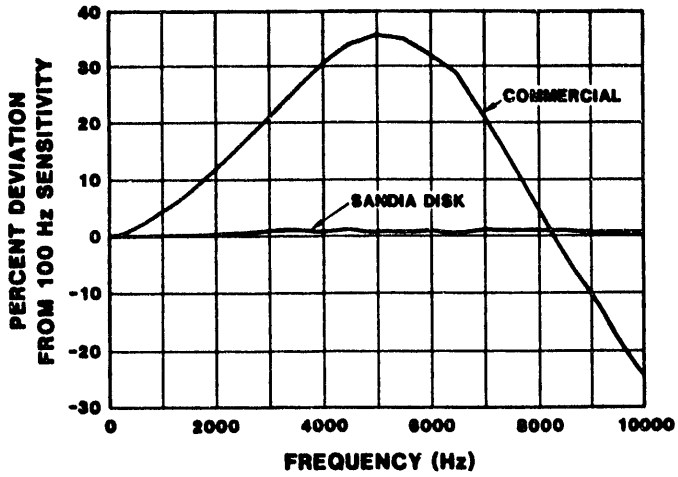

a) Shaker Calibration Comparison for Uniaxial and Commercial Isolators

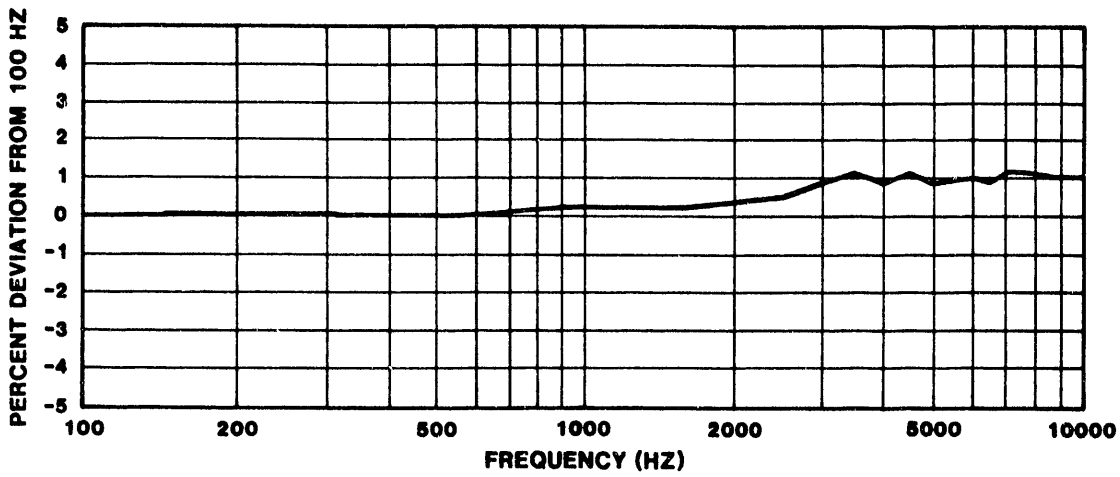

b) Shaker Calibration of Uniaxial Isolator

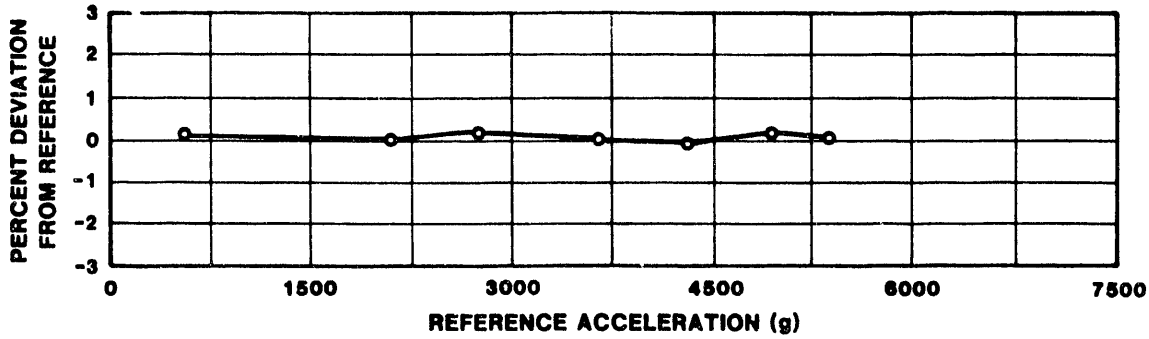

c) Dropball Calibration of Uniaxial Isolator

Figure 2: Calibrations for Commercial and Uniaxial Isolators

uniaxial technique and one axis of the triaxial isolation technique are tested with the normal input. The other two axes of the triax are characterized with a transverse input created by the Hopkinson bar configuration in Figure 4. A transverse input is perpendicular to the mounting stud or parallel to the mounting surface. An in-axis response is the response of an accelerometer whose sensitive axis is in the direction of the shock. An out-of-axis response is the response of an accelerometer whose sensitive axis is not in the direction of the shock. The uniaxial isolation technique and one axis of the triaxial isolation technique have in-axis response for a normal input. Each of the two other orthogonal axes of the triaxial isolation technique can have in-axis response for a transverse input.

These two Hopkinson bar configurations are used to characterize the response of the isolation techniques in both the time domain as a sensitivity calculation and in the frequency domain as frequency response functions. The sensitivity calculation is described below. The frequency response functions are calculated in the same manner as reported previously [6] except that an accelerometer mounted on the end of the bar is used as the reference acceleration for transverse inputs.

The theory of stress wave propagation in a Hopkinson bar is well documented in the literature [9,10]. The results of this theory are summarized as follows:

A Hopkinson bar is defined as a perfectly elastic, homogeneous bar of constant cross-section.

A stress wave will propagate in a Hopkinson bar as a one-dimensional elastic wave without attenuation or distortion if the wavelength, λ, is large relative to the diameter, D, or $10D \leq \lambda$.

For a one-dimensional stress wave propagating in a Hopkinson bar, the motion of a free end of the bar as a result of this wave is:

$$v = 2c\varepsilon \tag{1}$$

or,

$$a = 2c\left[\frac{d\varepsilon}{dt}\right] \tag{2}$$

where v and a are the velocity and acceleration, respectively, of the end of the bar, $c=\sqrt{E/\rho}$ is the wave propagation speed in the bar, E is the modulus of elasticity, ρ is the density for the Hopkinson bar material, and ε is the strain measured in the bar at a location that is not affected by reflections during the measurement interval.

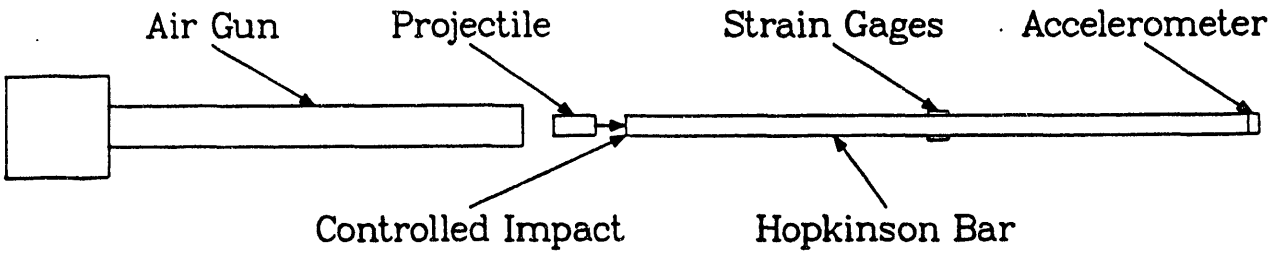

Figure 3: Hopkinson Bar Configuration for Normal Input.

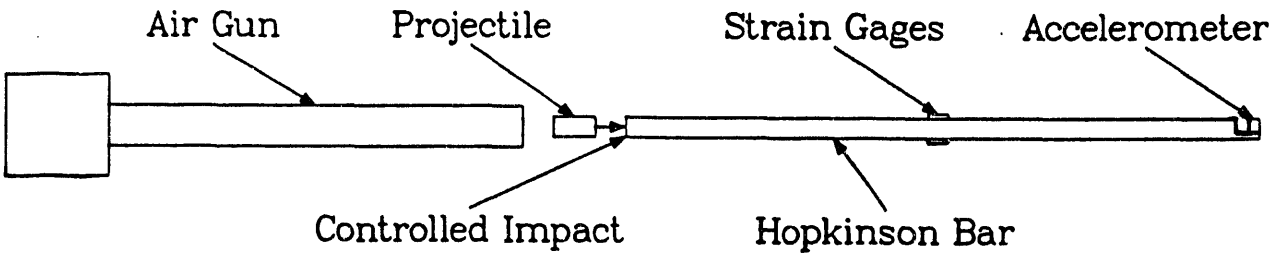

Figure 4: Hopkinson Bar Configuration for Transverse Input.

The motion of an accelerometer mounted on the end of the bar will be governed by equations (1) and (2) if the mechanical impedance of the accelerometer is much less than that of the bar or if the thickness of the accelerometer is much less than the wavelength. The requirement on the strain gage is that the gage length (g.l.) be less than the wavelength or $\lambda \geq 10$ g.l.

The Shock Laboratory Hopkinson bar, used for accelerometer testing, is shown schematically in Figures 3-4 and is made of 6 Al, 4 V titanium alloy (6% aluminum and 4% vanadium) with a 72 inch length and a 0.76 inch diameter. The bar is supported in a way that allows it to move freely in the axial direction. A low pressure air gun is used to fire a 2 inch long hardened tool steel projectile at the end of the bar. This impact creates a stress pulse which propagates toward the opposite end of the Hopkinson bar. The amplitude of the pulse is controlled by regulating the air gun pressure, which determines the impact speed. The shape (approximately a half sine) and duration of the pulse are controlled by placing various thicknesses of paper (3x5 index cards) on the impact surface. The two strain gages are located 49.75 inches from the end on which the accelerometer is mounted and are mounted at diametrically opposite positions on the bar. The 49.75 inch

strain gage location is in the mid-portion of the bar and allows a longer incident pulse, if desired. These gages are connected in opposite arms of a Wheatstone bridge to measure the net axial strain.

Once recorded, the strain and acceleration records can be compared by using either velocity or acceleration as shown in (1) and (2). When these comparisons are made, the time delay of the acceleration record, which is equal to the time for the wave to propagate from the strain gage to the end of the bar, must be taken into account. Hopkinson bar accelerometer calibration methods documented in the literature [11-13] generally use velocity, in which case the accelerometer record is integrated and compared directly to the strain record converted to velocity by the factor 2c. This provides smooth curves for comparison of time histories, however much of the higher frequency information is lost due to the integration process. Since it was desired to preserve the frequency response of the data, acceleration is used for the comparison of the data. Consequently, the time derivative of the strain records was required, and the resulting signal may be contaminated by high frequency noise created in the process of calculating the derivative. This problem was essentially eliminated by: 1) adequate sample rate of 500 kHz or higher; 2) low pass digital filtering with a cutoff frequency well above the frequency range of interest (10 kHz); and most importantly, 3) an accurate differentiation algorithm which was derived using the Fourier series reconstruction techniques in [14]. This algorithm results in an exact derivative of the digitized signal providing the Sampling Theorem has not been violated, that is, the data is not aliased [15].

The selected technique for calculating the sensitivity change at temperatures other than ambient, using the acceleration derived from the Hopkinson bar strain measurements, can be used only to estimate the change in sensitivity due to temperature because of the uncertainties associated with the measurements. Most of the errors are deterministic and will be cancelled when the percentage sensitivity change due to the -50°F temperature is calculated in the following equation [8]:

$$C = \left[\frac{A_{Ac-50}}{A_{Ac-A}} \cdot \frac{A_{Hop-A}}{A_{Hop-50}} - 1 \right] \times 100 \qquad (3)$$

where:

C = Percentage sensitivity change at -50°F as compared to ambient,

A_{Ac-50} = Shock amplitude measured by accelerometer at -50°F,

A_{Ac-A} = Shock amplitude measured by accelerometer at ambient,

A_{Hop-A} = Shock amplitude derived from strain gages for ambient test, and

A_{Hop-50} = Shock amplitude derived from strain gages for -50°F test.

A similar equation is used for the sensitivity change at +186°F.

UNIAXIAL ISOLATION TECHNIQUE PERFORMANCE

Twelve piezoresistive accelerometers mounted in the uniaxial isolation technique were used to assess the performance of the technique at -50°F and +186°F. Each accelerometer was subjected to five 5000 g pulses with a duration of 100 μs at each of five temperatures: ambient (70°F), -50°F, ambient, +186°F, and ambient. The accelerometers were tested at ambient after each test at a temperature extreme because the temperatures of -50°F and +186°F are beyond the manufacturer's operational range, -30°F to +150°F. The last ambient test ensured that the accelerometer was still operational after exposure to the extreme temperature environment.

The uniaxial isolation technique was characterized in the time domain with equation (2). The data from the strain gages and the accelerometers were digitally filtered at 17 kHz prior to the sensitivity calculation. The average sensitivity change at -50°F was 6.0% or -0.05%/°F. The average sensitivity change at +186°F was -4.3% or -0.04%/°F. These results are lower than the -0.06%/°F quoted in the manufacturer's specifications.

An acceleration-to-acceleration frequency response function was calculated for the uniaxial isolation technique at the two temperature extremes and compared to the frequency response function at ambient temperature. The calculations were made in the same manner as those published previously [6], and the frequency resolution for these calculations is 244 Hz. The magnitudes of the frequency response functions are shown in Figure 5 which shows that the magnitudes at 10 kHz deviate less than 10 percent from the magnitude at low frequency for all three temperature conditions. The frequency response function phase (not shown) varies in an approximately linear manner up to 10 kHz for all three temperature conditions. The deviation in the frequency response function magnitude above 20 kHz can be explained by the coherence functions (not shown) which show the coherence between the input and the output accelerations is less than one above 20 kHz. The computational anomaly, indicated by the lack of coherence, creates an apparent resonance above 20 kHz that is not a mechanical resonance in the uniaxial isolation technique.

TRIAXIAL ISOLATION TECHNIQUE PERFORMANCE

The triaxial isolation assembly, using a beryllium block, has been characterized at both ambient and at -50°F. Two beryllium triaxes were characterized at two levels: 2500 g and 5000 g, but only the results for the 5000 g input are shown here. The 2500 g results are similar. Each accelerometer in each triax was subjected to five 2500 g, 70 μs pulses and to five 5000 g, 70 μs pulses at the two temperatures: ambient (70°F) and -50°F.

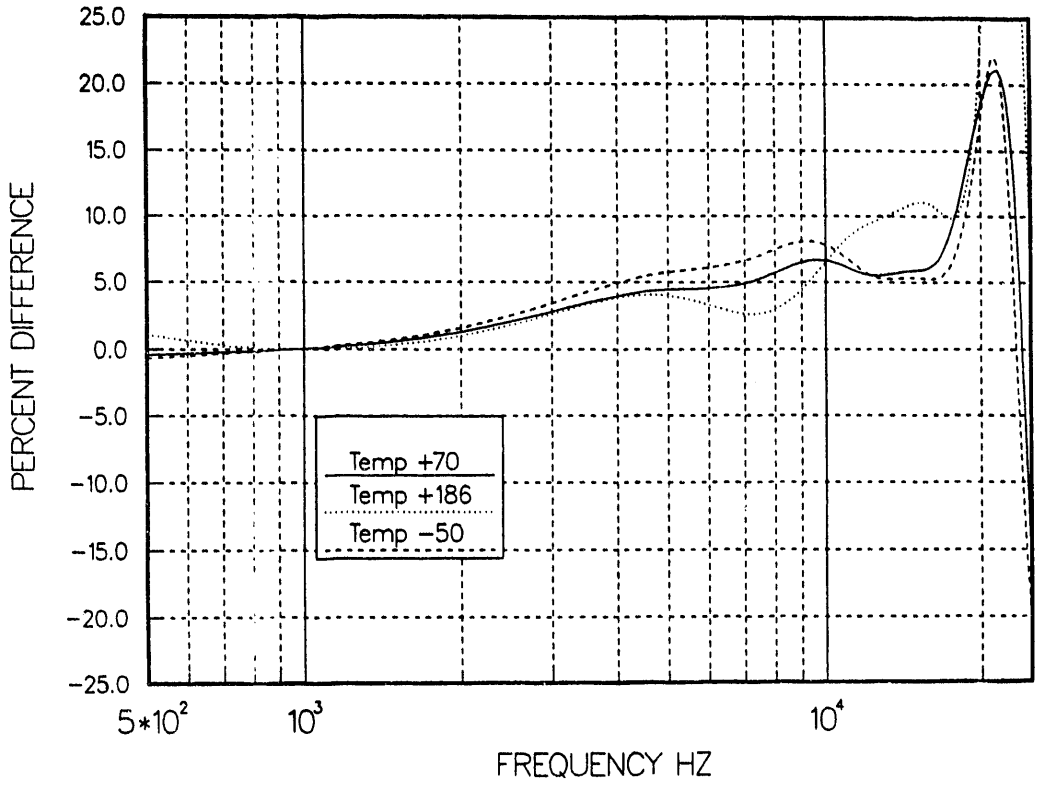

Figure 5: Frequency Response Function Magnitude for the Uniaxial Isolation Technique at -50°F, Ambient (70°F), and +186°F with a 5000 g, 100 μs Input Pulse.

The data from the strain gages and the accelerometers were digitally filtered at 25 kHz prior to the calculations. Sensitivity changes were calculated for the ten pulses applied to each accelerometer and averaged. The changes range from -0.05 %/°F to -0.11 %/°F and are generally higher than the -0.06%/°F quoted in the manufacturer's specifications. At this point, the calculated change is applied to each individual accelerometer until more data can be accumulated for an average sensitivity change calculation.

Frequency response function magnitudes for the triax at ambient are shown in Figure 6 for both the normal input and the transverse input. Frequency response functions for the triax at -50°F are shown in Figure 7 for both the normal input and the transverse input. Phase and coherence functions were also calculated but are not shown. The phase is approximately linear over the 10 kHz bandwidth, and the coherence is one until about 20 kHz which causes the large deviations in the magnitudes shown in Figures 6-7. The phase changes more for the transverse input than for the normal input over the 10 kHz bandwidth.

The triaxial isolation technique with a 7075 aluminum block has also been tested but generally has acceptable performance over a more limited frequency bandwidth, about 4 kHz, than the beryllium. Additionally, the screws in the

aluminum blocks loosen more easily, and there is more out-of-axis response for the aluminum triax. The out-of-axis response is increased in the aluminum block because it has a resonance at about the same frequency as the resonance of the 20,000 g piezoresistive accelerometers mounted in the triax, 350 kHz. The beryllium is stiffer and less dense, so its first resonance is in excess of 400 kHz and does not excite the accelerometer's resonance.

The attachment of the triax to the bar was critical with the Hopkinson bar configuration for a transverse input. The triax was bolted to the Hopkinson bar at the lower acceleration levels, but at input acceleration levels of about 4000 g and above, the triax had to be bolted and glued to the bar. With the bolt and the glue, the triax was prevented from moving with respect to the Hopkinson bar surface during the application of the input acceleration pulse. Additionally, there was a difference in the response of the out-of-axis transverse accelerometers that seems to be dependent upon their orientation. As can be seen in Figure 1, the two transverse accelerometers are not oriented the same way; they are oriented at 90° to each other. The out-of-axis response was generally about 10% if the shock passed across the long dimension of the accelerometer. If the shock passed across the short dimension of the accelerometer, the out-of-axis response was somewhat larger (about 50%) and appeared to contain more excitation of the accelerometer's resonance.

Finally, a comparison of the Fourier transforms for a hard mounted accelerometer and one axis of the triaxial isolation technique is shown in Figure 8 for a 5000 g, 70 μs input pulse on the Hopkinson bar. Figure 8 shows that the triaxial isolation technique has attenuated the accelerometer resonance by a factor of three and, therefore, has successfully isolated the accelerometer from high frequency input.

HOPKINSON BAR CALIBRATION RESULTS

Three separate operations were performed to calibrate the Hopkinson bar. First, a calculation of the wave speed for the titanium Hopkinson bar was made at the temperatures of -50°F and +160°F. Secondly, a reference accelerometer, calibrated by NIST traceable standards, was placed on the end of the bar in the same manner as the accelerometers for the calibration tests and was subjected to shock pulses at various amplitudes. The reference accelerometer output was compared to the acceleration calculated from the Hopkinson bar strain gage response. Lastly, a static load test was performed on the Hopkinson bar; and an effective gage factor was calculated from the measured bar sensitivity.

The stress wave speed in the Hopkinson bar is an important quantity because it occurs in the the Hopkinson bar acceleration calculation as shown in (1) and (2). The stress wave speed is calculated from material properties as:

$$c = \sqrt{\frac{E}{\rho}} \qquad (4)$$

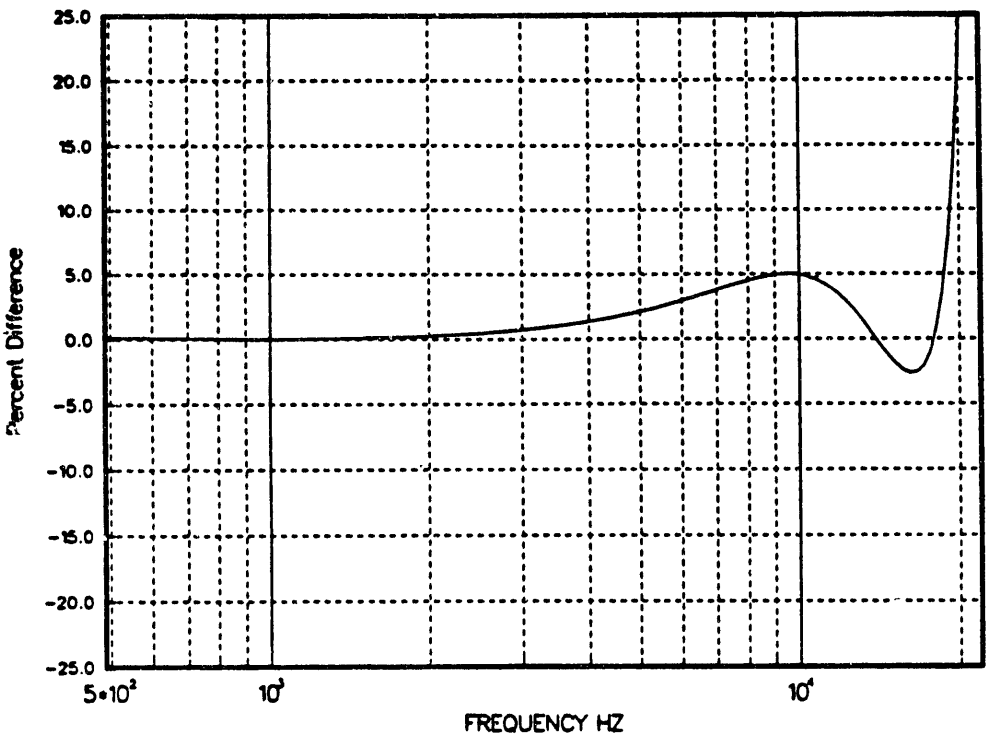

a) Normal Input

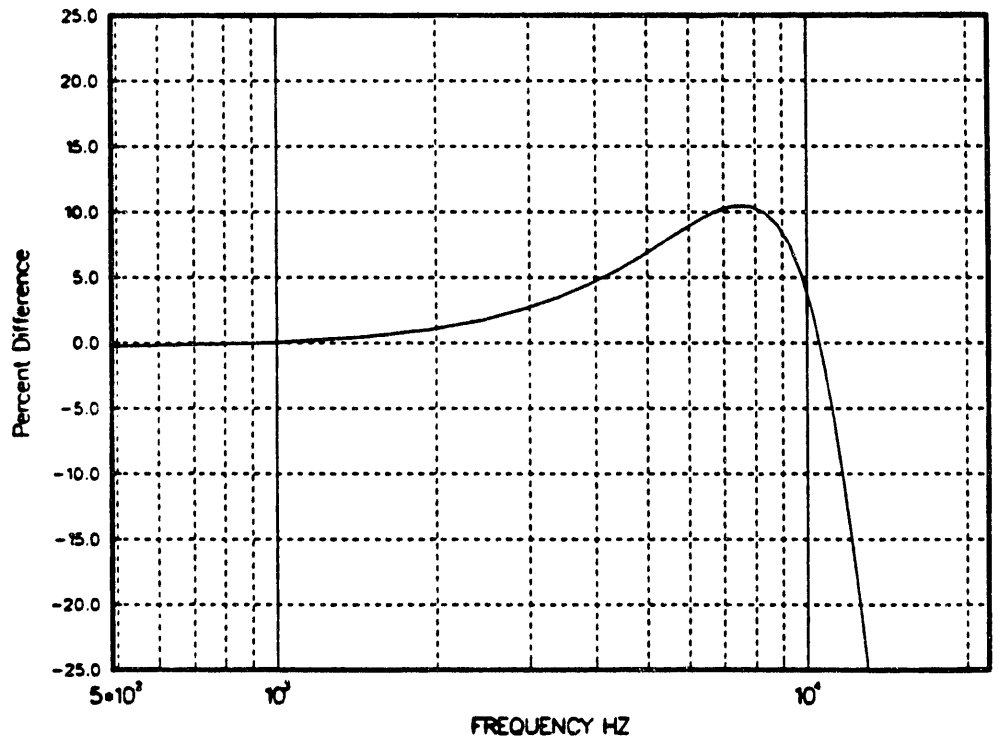

b) Transverse Input

Figure 6: Frequency Response Function Magnitude for the Triaxial Isolation Technique at Ambient (70°F) with a 5000 g, 70 μs Input Pulse.

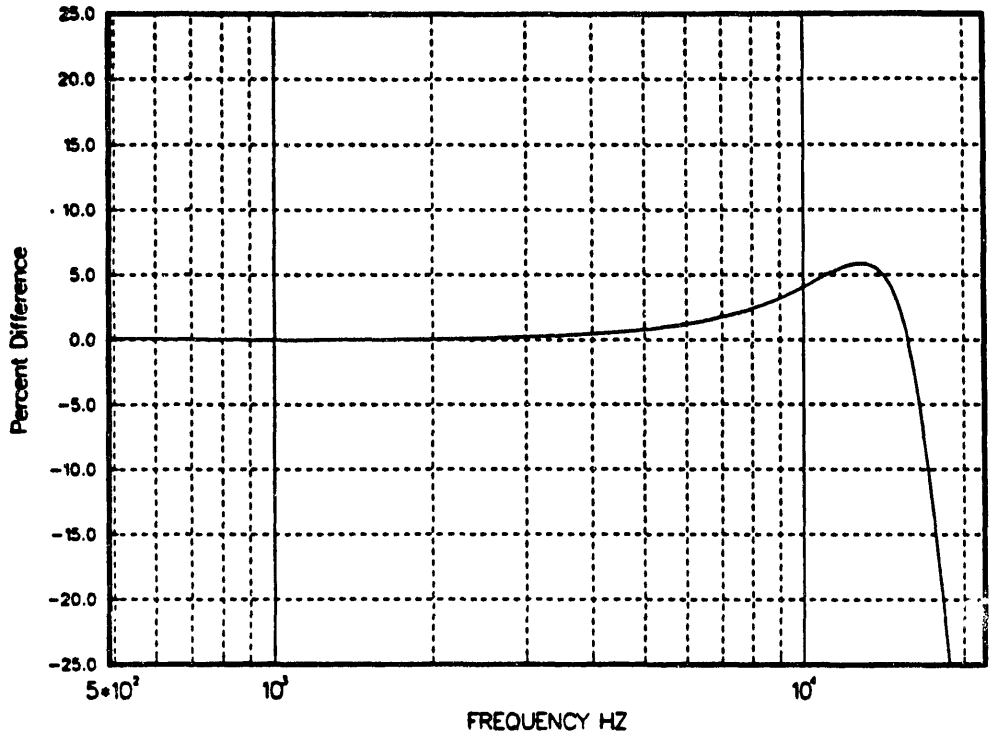

a) Normal Input

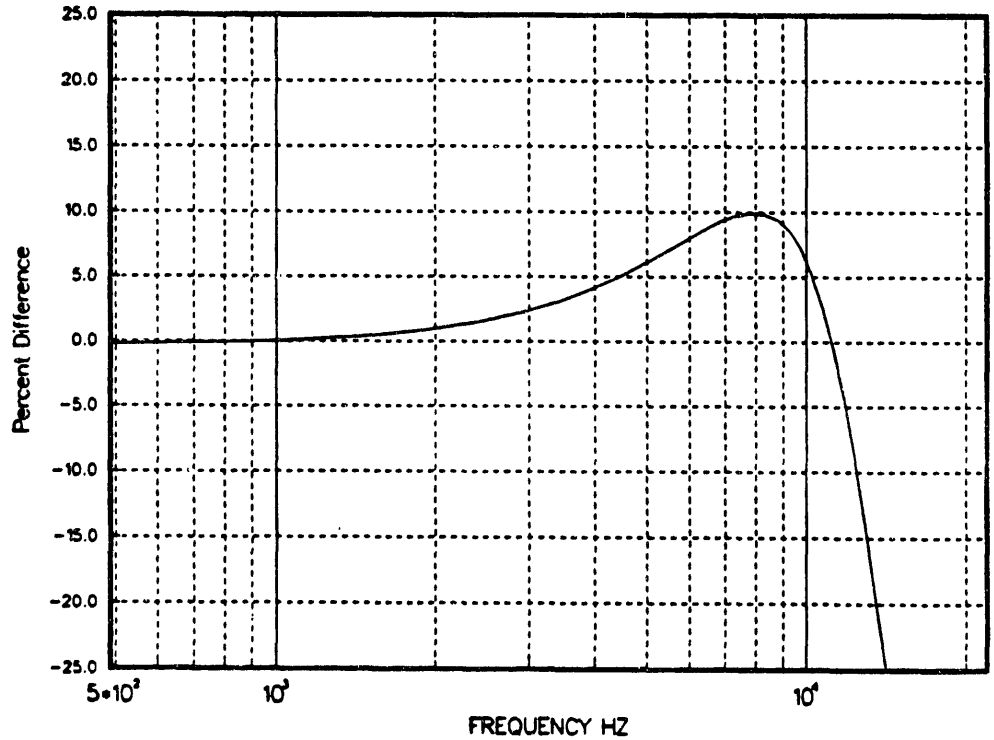

b) Transverse Input

Figure 7: Frequency Response Function Magnitude for the Triaxial Isolation Technique at -50°F with a 5000 g, 70 μs Input Pulse.

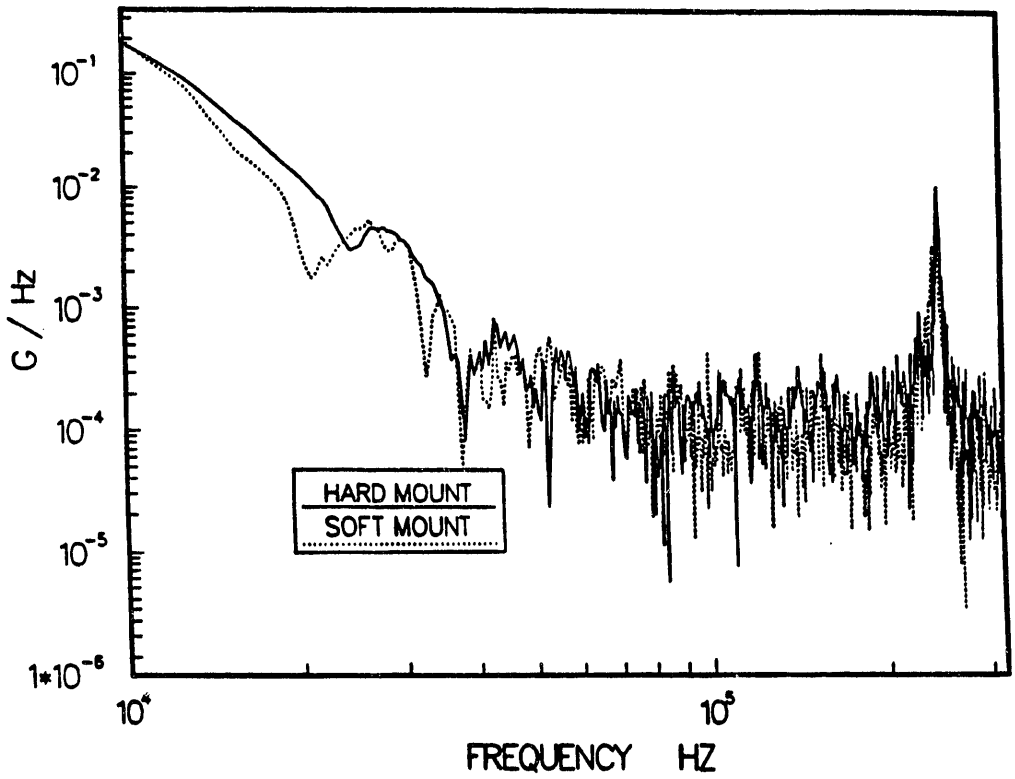

Figure 8: Comparison of Fourier Transforms for a Hard Mounted Accelerometer and One Axis of the Triaxial Isolation Technique with a 5000 g, 70 μs Pulse Input.

where E is the modulus of elasticity and ρ is the density for the Hopkinson bar material. The modulus varies between 102% @-50°F and 97% @+165°F of the nominal value, 16×10^6 psi [16]. The change in density is 0.0015% at either of the temperature extremes and is negligible [16]. The nominal stress wave speed for titanium is 196,210 in/sec. At the cold temperature, the wave speed will increase by $\sqrt{1.02}$ or 1.00995 (1%) in the length of the bar that is inside the temperature chamber, about 2 in. Since the round trip time to the strain gages is measured for the stress wave speed, the stress wave travels twice that distance or 4 in. at about 5 μs/in. It takes 20 μs for the stress wave to traverse this distance. An upper bound for the increase in this time due to the cold temperature is 1% of 20 μs or 0.2 μs. Since the highest resolution available with Shock Laboratory instrumentation is 0.5 μs, this increase in the stress wave speed cannot be measured at -50°F. A similar argument can be made for the decrease in wave speed at the hot temperature; the decrease is about 2% over the 4 in. bar length or 0.4 μs. Again, this change in the wave speed will not be detected with current instrumentation time resolution. These calculations were verified with Hopkinson bar measurements, and consequently, the stress wave speed was not changed for accelerometer calibrations performed at -50°F or +160°F.

A Kistler 805A reference accelerometer (S/N 1886) was used for the second part of the Hopkinson bar evaluation. The 805A has a NIST-traceable

calibration, for both shock and vibration. The 805A was placed on the Hopkinson bar in Figure 3 in the same manner as the accelerometers calibrated. The response of the 805A was compared to the acceleration derived from the strain gages on the bar using a frequency response function. For a nominal pulse duration of 100 μs and three shock levels (4000 g, 10000 g, and 15000 g), an ensemble of five pulses was applied to the reference accelerometer. An example of a shock pulse with its corresponding Fourier transform magnitude measured by the strain gages is shown in Figure 9. Considerable preparation of the Hopkinson Bar data was required before

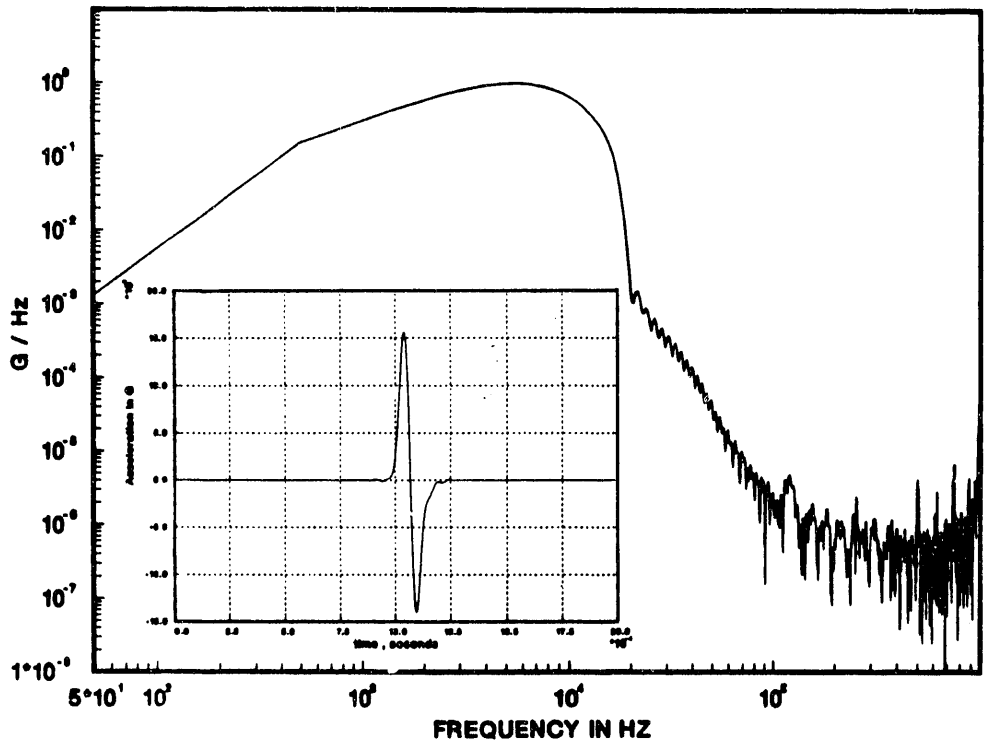

Figure 9: Fourier Transform Magnitude for 15000 G Pulse.

frequency response functions could be calculated. Since an acceleration response to acceleration input frequency response function was desired, the strain data was converted to velocity according to (1). The velocity data were digitally filtered with a ten-pole Butterworth filter whose cutoff frequency of 17 kHz was chosen to reduce the noise created in taking the derivative to obtain the acceleration. The data were filtered in both the forward and backward directions to remove the filter phase shift. The 17 kHz cutoff frequency was determined from an examination of the Fourier transform magnitude. The cutoff frequency for the filter was chosen based on two criteria: 1) the frequency at which the pulse transform becomes noise and 2) the frequency at which the coherence, computed using an ensemble average, between the input and response accelerations deviated from unity. The filter cutoff frequency was chosen higher than the second frequency so that the filter attenuation did not affect the coherent frequency range. Input

acceleration was calculated by taking the derivative of the velocity as described in the previous section. The resultant input acceleration was then shifted in time to account for the wave transit time from the strain gage to the accelerometer assembly. Several tests were performed to determine the correct time shift which was measured as 261 μs. This value is one half the time for the stress wave to travel to the end of the bar and back to the strain gages. The resulting input acceleration data as well as the response data were filtered at 40 kHz with a ten pole Butterworth digital filter in both a forward and backward directions to eliminate filter phase shift and then windowed. A boxcar window tapered with Blackman-Harris cosine functions was applied to prevent leakage errors. The effects of the window and the filter were examined closely to assure that they did not produce any contamination of the data. The magnitude and phase of the frequency response functions, with Hopkinson bar as input and the reference accelerometer as output, were calculated so that a quantitative evaluation could be made of the Hopkinson bar as compared to the reference accelerometer [8]. The frequency response functions for the three different acceleration inputs are shown in Figure 10. Also shown in Figure 10 is the variation of the reference accelerometer sensitivity as a function of frequency for a vibration calibration since the shock calibration data was not available. The senstivity values from the shock calibration and the vibration calibration at 1000 Hz are the same. Each curve is plotted as percent difference from the 1000 Hz value for that curve. The 1000 Hz value was chosen because of noise problems at lower frequencies. The maximum deviations of the Hopkinson bar frequency response functions from the reference accelerometer curve are -1% and +5% at 10 kHz.

A static force calibration, to determine an effective gage factor of the titanium bar, was undertaken as the last part of the certification effort. The bar was placed vertically in a load test machine, manufactured by MTS, and was loaded with a 500 lb compressive load in 50 lb increments. The output of the strain gages was compared to a NIST-traceable calibrated load cell, and a sensitivity for the strain gage, S_{sg}, was calculated in μv/v/lb. The indicated force, F_1, from the bar is then:

$$F_1 = \frac{V_{out}}{S_{sg}\ V_e} \tag{5}$$

where V_{out} is the output voltage from the strain gages as the load is applied and V_e is the excitation voltage on the strain gage bridge. This force, F_1, may be compared to the force measured on the bar, F_2, in response to a shock pulse:

$$F_2 = \frac{2\ E\ A\ V_{out}}{G_f\ V_e} \tag{6}$$

where G_f is the gage factor, E is the modulus of elasticity, and A is the bar cross-sectional area. F_1 and F_2 are set equal to each other in order to

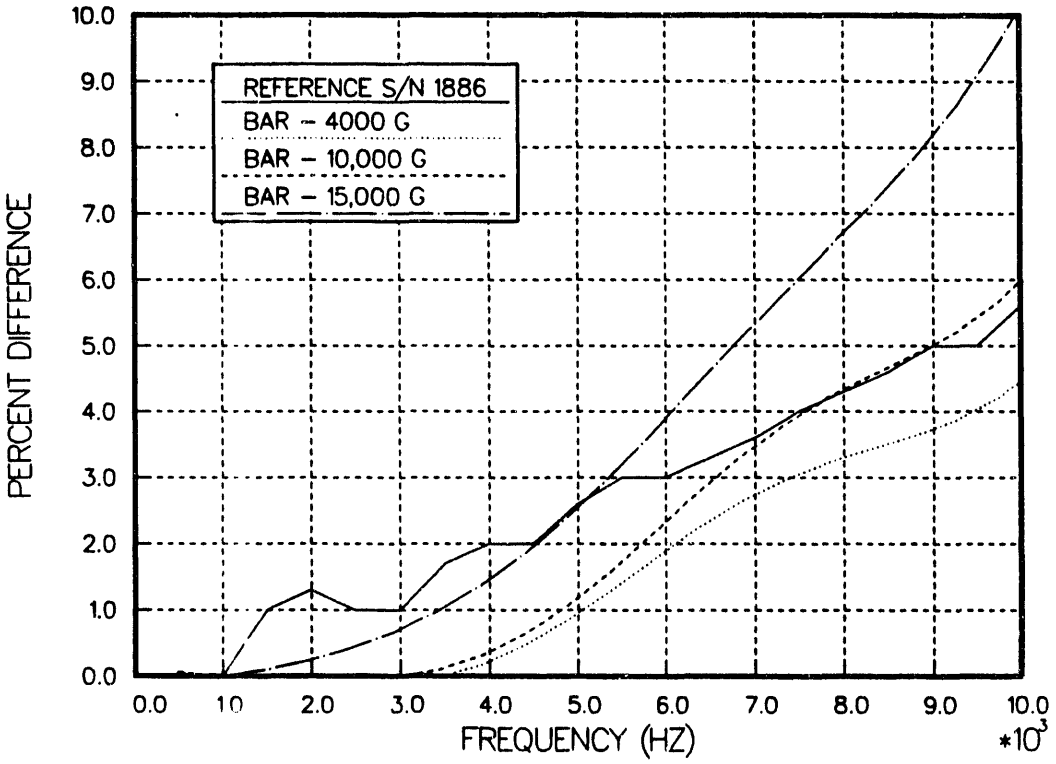

Figure 10: Reference Accelerometer and Hopkinson Bar Frequency Response Functions.

calibrate the output F_2. After common quantities are cancelled, the equality becomes an expression for an equivalent gage factor as:

$$G_f = 2 \cdot E \cdot A \cdot S_{sg} \qquad (7)$$

which has a numerical value of 2.07. This value is 3% lower than the manufacturer's specified value of 2.135. An examination of the numerical values for the frequency response functions, instead of the percent difference shown in Figure 5, reveals that the values at 1000 Hz are ≈1.03 for all three functions. That is, the reference accelerometer is 3% higher than the acceleration derived from the Hopkinson bar which agrees with the 3% lower equivalent gage factor derived from the load test. The peak acceleration values for the Hopkinson bar with a gage factor decreased by 3% and for the reference acclerometer are given in the table below.

The Kistler Model 805A accelerometer, S/N 1886, was calibrated at shock levels of 1000 g, 3000 g, and 10,000 g using traceable, fundamental length and time measurements and certified by the Sandia Primary Standards Laboratory. Their estimate of the uncertainty is +5% of reading (File #4092F). Peak acceleration calculated from the bar data agreed with the peak calculated from the reference accelerometer, 1000 Hz, sensitivity within the +5% uncertainty. The differences averaged 4.3% (three standard deviations = 0.6%) at 4000 g and 1.6% (three standard deviations = 1%) at 10,000 g and

COMPARISON OF CORRECTED HOPKINSON BAR ACCELERATION VALUES WITH REFERENCE ACCELEROMETER

Nominal Peak Value	Corrected Hopkinson Bar Peak Acceleration	Reference Peak Acceleration	Percent Difference
4000 g	4016 g	4189 g	4.1%
	4233 g	4425 g	4.3%
	4044 g	4220 g	4.2%
	4207 g	4402 g	4.4%
	4042 g	4237 g	4.6%
10000 g	10100 g	10240 g	1.4%
	10180 g	10380 g	1.9%
	10370 g	10530 g	1.5%
	10150 g	10360 g	2.0%
	9825 g	9977 g	1.5%
15000 g	16050 g	16320 g	1.7%
	15680 g	15930 g	1.6%
	16590 g	16920 g	2.0%
	14900 g	15080 g	1.2%
	15860 g	16040 g	1.1%

15,000 g. The sum of the reference uncertainty and the maximum of the three standard deviations were added to obtain the estimated uncertainty of 6%. It is felt that the uncertainty should not change as long as the bar suffers no physical damage and the strain gages are not changed.

CONCLUSIONS AND FUTURE WORK

Uniaxial and triaxial isolation techniques for a piezoresistive accelerometer have been characterized over a bandwidth of DC to 10 kHz with a Hopkinson bar. The uniaxial shock isolation technique has demonstrated acceptable characteristics for a temperature range of -50°F to +186°F, and the triaxial shock isolation technique has demonstrated acceptable results for a temperature range of -50°F to 70°F for this bandwidth of DC to 10 kHz. The Hopkinson bar has been certified with a transfer standard with an uncertainty of 6%. The frequency bandwidth for these characterizations and certifications will be extended to 30-50 kHz by the use of a beryllium Hopkinson bar instead of the titanium bar used in these studies. Additionally, characterization of the piezoresistive accelerometer's cross-axis sensitivity, with and without a mechanical isolator, will be studied using the beryllium bar. The low Poisson's ratio and the high stress wave speed for the beryllium will allow these studies.

REFERENCES

1. V. I. Bateman, T. G. Carne, D. L. Gregory, S. W. Attaway, H. R. Yoshimura, "Force Reconstruction for the Slapdown Test of a Nuclear Transportation Cask," ASME Journal of Vibration and Acoustics, Vol. 113, No. 2, 4/91.
2. V. I. Bateman, T. G. Carne, and D. M. McCall, "Force Reconstruction for Impact Tests of an Energy-Absorbing Nose," The International Journal of Analytical and Experimental Modal Analysis, Vol. 7, No. 1, January 1992.
3. D. K. Overmier and M. J. Forrestal, "Experiment for Evaluation of Acceleration Measurement Capability," AIAA Journal, Vol. 13, No. 9, pp.1234-1236, September 1975.
4. D. K. Overmier and P. L. Walter, "A Shock-Isolated Package for an Earth Penetrator Instrumentation System: Design Analysis and Test Results," SAND80-1197, Sandia National Laboratories, October 1980.
5. V. I. Bateman and O. M. Solomon, Jr., "Characterization of Accelerometer Mountings in Shock Environments," SAND86-1606, August 1986.
6. Bateman, V. I., R. G. Bell, and N. T. Davie, "Evaluation of Shock Isolation Techniques for a Piezoresistive Accelerometer," Proceedings of the 60th Shock and Vibration Symposium, David Taylor Research Center, Portsmouth, VA, November 1989.
7. V. I. Bateman, R. G. Bell, F. A. Brown, N. T. Davie, and M. A. Nusser, "Evaluation of Uniaxial and Triaxial Shock Isolation Techniques for a Piezoresistive Accelerometer," Proceedings of the 61st Shock and Vibration Symposium, Vol. IV, October 1990, pp. 161-170.
8. V. I. Bateman, W. B. Leisher, F. A. Brown, and N. T. Davie, "Calibration of a Hopkinson Bar With a Transfer Standard," Proceedings of the 62nd Shock and Vibration Symposium, Vol. III, October 1991, pp. 568-577.
9. R. Davies, "A Critical Study of the Hopkinson Pressure Bar," Philosophical Transactions, Series A, Royal Society of London, Vol. 240, pp. 352-375, January 8, 1948.
10. H. Kolsky, Stress Waves in Solids, Oxford University Press, 1953.
11. J. Cannon and D. Rimbey, "Transient Method of Calibrating a Piezoelectric Accelerometer for the High g-level Range," American Society of Mechanical Engineers No. 71-Vibr-43, ASME Vibrations Conference and the International Design Automation Conference, September 1971, Toronto, Canada.
12. G. Brown, "Accelerometer Calibration with the Hopkinson Pressure Bar," Instrument Society of America preprint No. 49.3.63, 18th Annual ISA Conference and Exhibit, September 1963, Chicago, Illinois.
13. R. D. Sill, "Shock Calibration of Accelerometers at Amplitudes to 100,000 g Using Compression Waves," Proceedings of the 29th International Instrument Symposium, Albuquerque, NM, May 2-6, 1983, pp. 503-516.
14. S. D. Stearns, "Integration and Interpolation of Sampled Waveforms," SAND77-1643, Sandia National Laboratories, January 1978.
15. S. D. Stearns, Digital Signal Analysis, Hayden Book Company Inc., 1975, pp. 37-40.
16. Metallic Materials and Elements for Aerospace Vehicle Structures, MIL-HDBK-5E, June 1987, Section 5.4.1.18.

END

DATE
FILMED
8/11/93